Paper 8

HEAT TRANSFER FROM A WIRE IN THE CRITICAL REGION

By U. Grigull* and E. Abadzic*

This work deals with experimental results on boiling from a horizontal platinum wire, 0·1 mm in diameter, submerged in saturated liquids as carbon dioxide (CO_2) and Freon 13 (CF_3Cl) in the critical region. Three discrete regimes without steady transition could be observed: natural convection, nucleate boiling, and film boiling. Near the critical point particular flow patterns appeared in the rising vapour in film boiling: regular bubbles, vapour columns, and vapour hazes with garland-like boundaries. These flow patterns could be simulated in model experiments with liquids and were also photographed with a high-speed camera.

EXPERIMENTAL PROCEDURE

A PLATINUM WIRE of 0·1 mm in diameter was arranged horizontally in a pressure vessel made of non-corrosive steel. This cuvette had an inside height of 60 mm, an inside length of 150 mm, and an inside depth of 20 mm; two opposite long sides were provided with glass windows. Carbon dioxide (CO_2) (critical values $p_c = 73{\cdot}8$ bar, $\theta_c = 31{\cdot}1°C$) and Freon 13 (CF_3Cl) ($P_c = 38{\cdot}6$ bar, $\theta_c = 28{\cdot}8°C$), were used as test fluids and the test region covered normalized pressures p/p_c from 0·75 to 1. The test fluids were cleaned from oil-contaminations by multiple distillation. In order to measure the potential drop two potential leads, 100 mm apart, were welded to the heating wire. The heat flux and wire temperature were determined from this and the measured current. Digitally indicating instruments were used for electrical measurements. In all instances the liquid temperature was close to that of boiling.

EXPERIMENTAL RESULTS

Measured values of heat flux q for CO_2 and Freon 13 were plotted against the temperature difference $\Delta\theta = \theta_w - \theta_s$ (Nukiyama plot), where θ_w is the heating wire temperature and θ_s is the saturation temperature; θ_s was determined from the measured pressure of the system. In Figs 8.1 and 8.2 three discrete regimes with no steady transition can be observed: natural convection, nucleate boiling, and film boiling.

The MS. of this paper was first received at the Institution on 23rd October 1967 and in its revised form, as accepted by the Council for publication, on 26th January 1968. 33

* *Technische Hochschule München, 8 München 2, Germany.*

Natural convection

Cleaning the heated wire by annealing and the fluid by multiple distillation ensured excellent moistening of the wire. It could be heated above saturation temperature without bubble boiling setting in. The natural convection regime can be observed in the lower left-hand side of Figs 8.1 and 8.2. The possible superheating in CO_2, for example, amounted to $\Delta\theta = 2{\cdot}4$ degC at $p = 55{\cdot}7$ bar, and decreased to 0·1 degC at $p = 71{\cdot}2$ bar. Above this permissible superheating value nucleate boiling suddenly occurred with a considerable decrease in wire temperature. The nucleate boiling regime was retained when the heat flux was reduced below that original value at which boiling first set in. Only after a complete disconnection of the heating wire and a few minutes' break could the natural convection regime again be observed. The values measured for natural convection in CO_2 can be obtained by the equation

$$Nu = 0{\cdot}94(Gr.Pr)^{1/8} \quad . \quad . \quad (8.1)$$

The Nusselt number in this instance is defined by $Nu = qd/[\lambda(\theta_w - \theta_s)]$, where d (= 0·1 mm) is the diameter of the wire. The Grashof number, Gr, is also based on d; Pr is the Prandtl number. For natural convection all physical properties were taken at mean film temperature. Owing to the lack of necessary physical properties, measurements in Freon 13 could not be evaluated.

Nucleate boiling

The experimental results for nucleate boiling are shown in the upper left of Figs 8.1 and 8.2. The slightly bent curves are limited in their upper part by the maximum heat flux

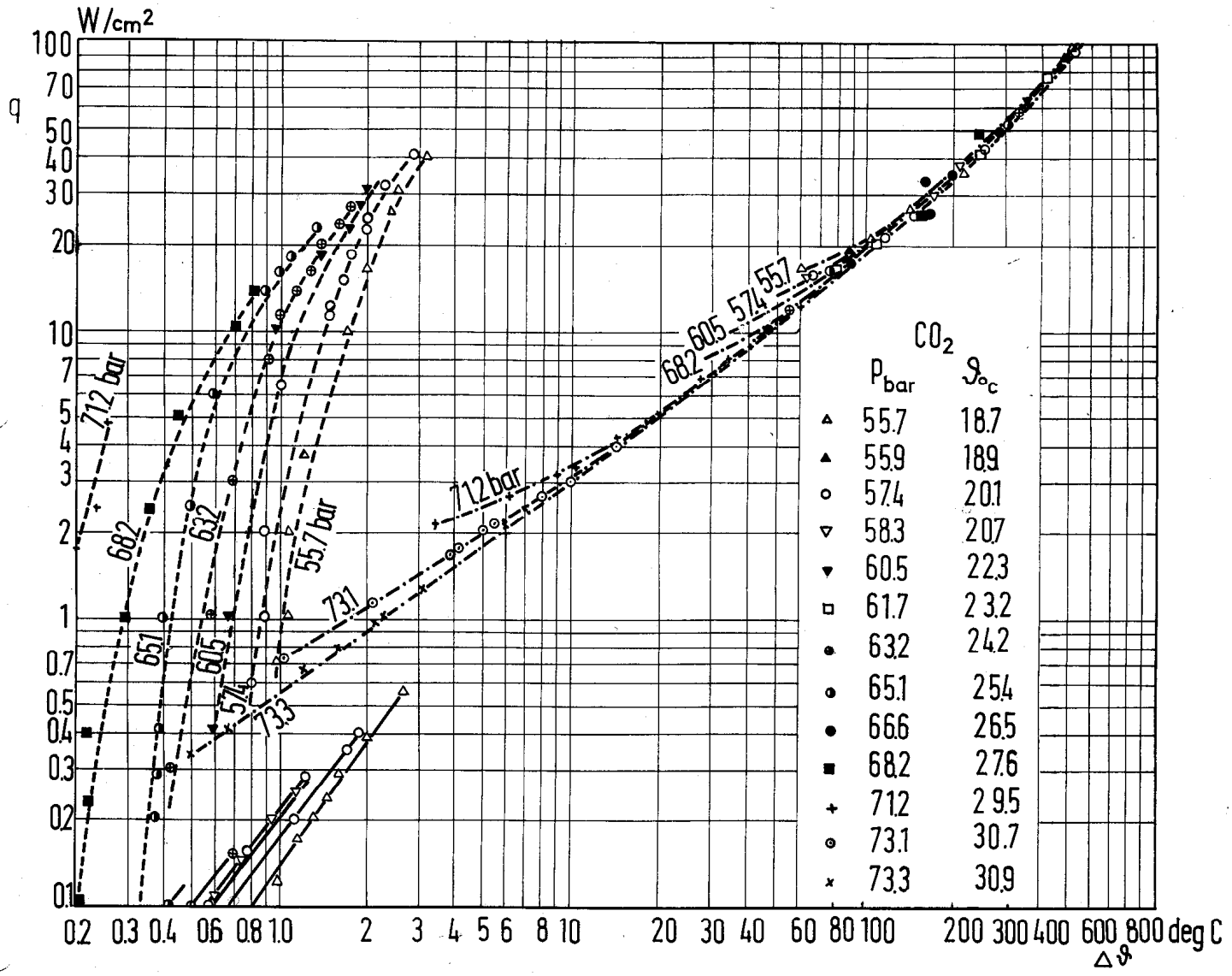

Fig. 8.1. Heat flux density q as a function of temperature difference $\Delta\theta = \theta_w - \theta_s$ for carbon dioxide

density, which is also known as the burn-out heat flux. This will be discussed in the following section.

In a linear plot of q versus wire temperature θ_w, using the saturation pressure p as a parameter, straight lines are obtained up to the value of q_{max}. This is shown for Freon 13 in Fig. 8.3. Very similar results are obtained for CO_2. The intersection of these straight lines with the abscissa indicates a wire temperature which we may call θ_0 and which is larger than or at least equal to the saturation temperature θ_s. The θ_s values are given as black dots on the abscissa of Fig. 8.3. If the heat transfer coefficient h is defined by the equation

$$h = q/(\theta_w - \theta_s) \quad . \quad . \quad . \quad (8.2)$$

the inclinations of the straight lines in Fig. 8.3 correspond to

$$h^* = q/(\theta_w - \theta_0) \geqslant h \quad . \quad . \quad . \quad (8.3)$$

Neglecting some scattering which is probably due to measuring uncertainties, h^* is constant in the entire region covered by Fig. 8.3. For Freon 13 a value of $h^* \approx 9{\cdot}5 \times 10^4$ W/m² degC is obtained, while $h^* \approx 21{\cdot}4 \times 10^4$ W/m² degC is found for CO_2. Dividing equation (8.3) by equation (8.2) results in

$$\frac{h}{h^*} = \frac{\theta_w - \theta_0}{\theta_w - \theta_s} = 1 - \frac{\theta_0 - \theta_s}{\theta_w - \theta_s} \quad . \quad . \quad (8.4)$$

The temperature difference $\theta_0 - \theta_s$ can be considered as that excess temperature at which bubbles begin to appear. It decreases with increasing pressure and assumes a value of zero at the critical pressure. The value of $\theta_0 - \theta_s$ as a function of pressure or saturation temperature resembles that of the surface tension, as is feasible from the physical meaning. Equation (8.4) demonstrates that the heat transfer coefficient h as a function of $1/(\theta_w - \theta_s)$ is linear with a negative, pressure-dependent slope. The portions on the co-ordinates correspond to h^* and $1/(\theta_0 - \theta_s)$. The value of h^* depends on the kind of liquid and the kind of geometry of the heating surface.

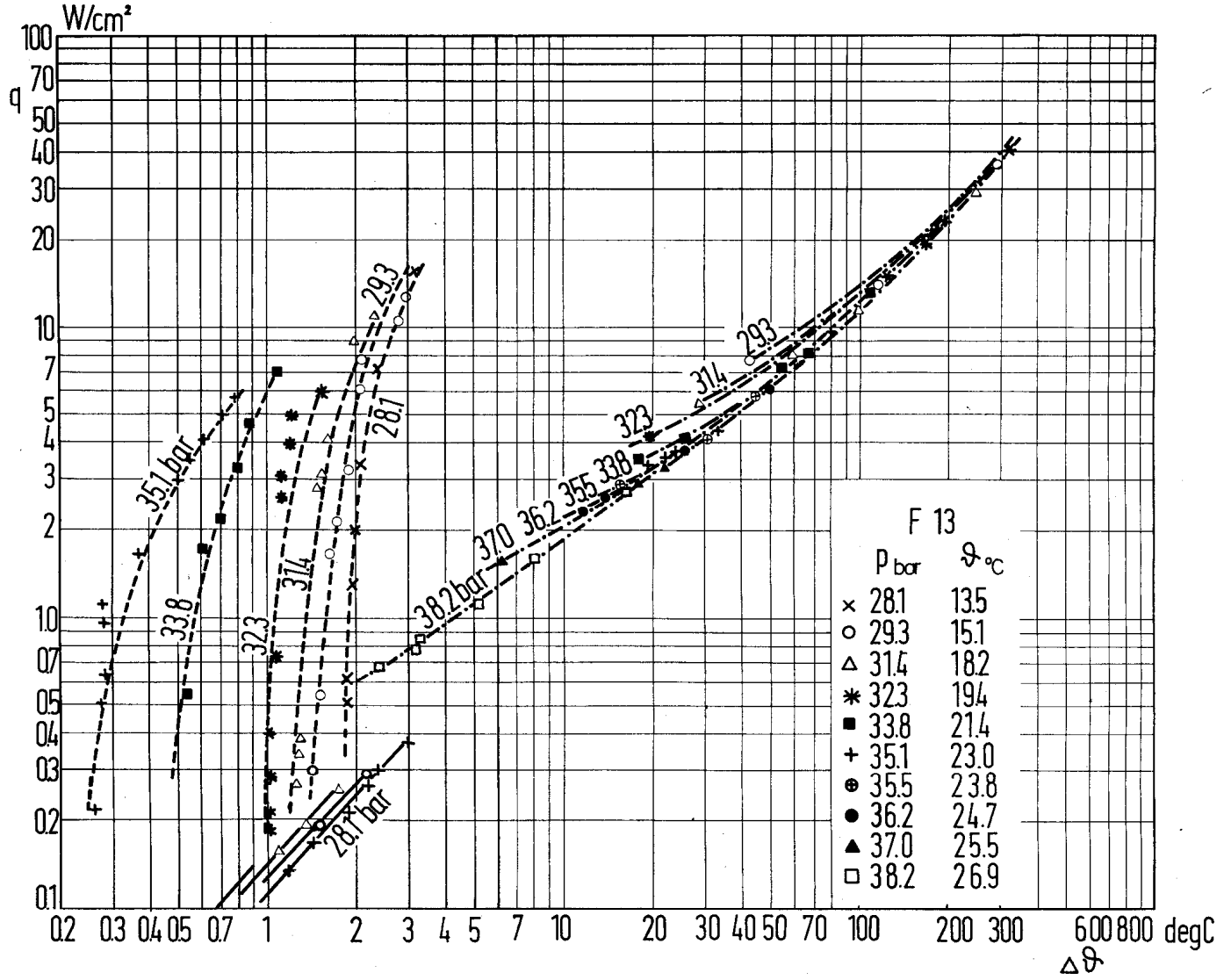

Fig. 8.2. Heat flux density q as a function of temperature difference $\Delta\theta = \theta_w - \theta_s$ for Freon 13

Film boiling

On the right of Figs 8.1 and 8.2 the experimental results for film boiling are presented. If the maximum heat flux density q_{max} is exceeded, film boiling will occur in the first instance in an arbitrary point of the heating wire and spread out rapidly along the entire heating wire. At pressures in the vicinity of the critical only, a vapour film is formed spontaneously along the entire length of the heating wire. If the heat flux is decreased during film boiling, spontaneous bubble boiling will set in at a certain value q_{min}. A steady transition region between film boiling and bubble boiling could not be observed in any of the experiments. The measured values of q_{max} and q_{min} are compiled in Table 8.1, which also gives the function M according to the definition

$$M = [(\rho' - \rho'')\sigma g]^{1/4} \rho''^{1/2} r \quad . \quad . \quad (8.5)$$

where ρ' and ρ'' are the saturation densities of the liquid and the vapour respectively, σ the surface tension, g the gravitational constant, and r the vaporization enthalpy. According to some authors (1)* (2) the quotient q_{max}/M is independent of pressure for horizontal, flat heating surfaces.

It is shown in Table 8.1 that such a relation is not accomplished for thin horizontal wires in the critical region of CO_2 and Freon 13; similarly it does not hold for q_{min}/M.

The influence of pressure on the q versus $(\theta_w - \theta_s)$ relation is significant only in the vicinity of q_{min} as shown in Figs 8.1 and 8.2. Outside this region the valid relation is

$$q = \text{const.}\ (\theta_w - \theta_s)^{3/4} \quad . \quad . \quad (8.6)$$

with the constant being independent of pressure and in agreement with a relation given by Bromley (3).

In the pressure region $0{\cdot}7 < p/p_c < 0{\cdot}9$ in film boiling, individual vapour bubbles detach from the heating wire and rise in regular patterns, occasionally in an arrangement like a chess-board (Fig. 8.4). In the pressure region

* *References are given in Appendix 8.1.*

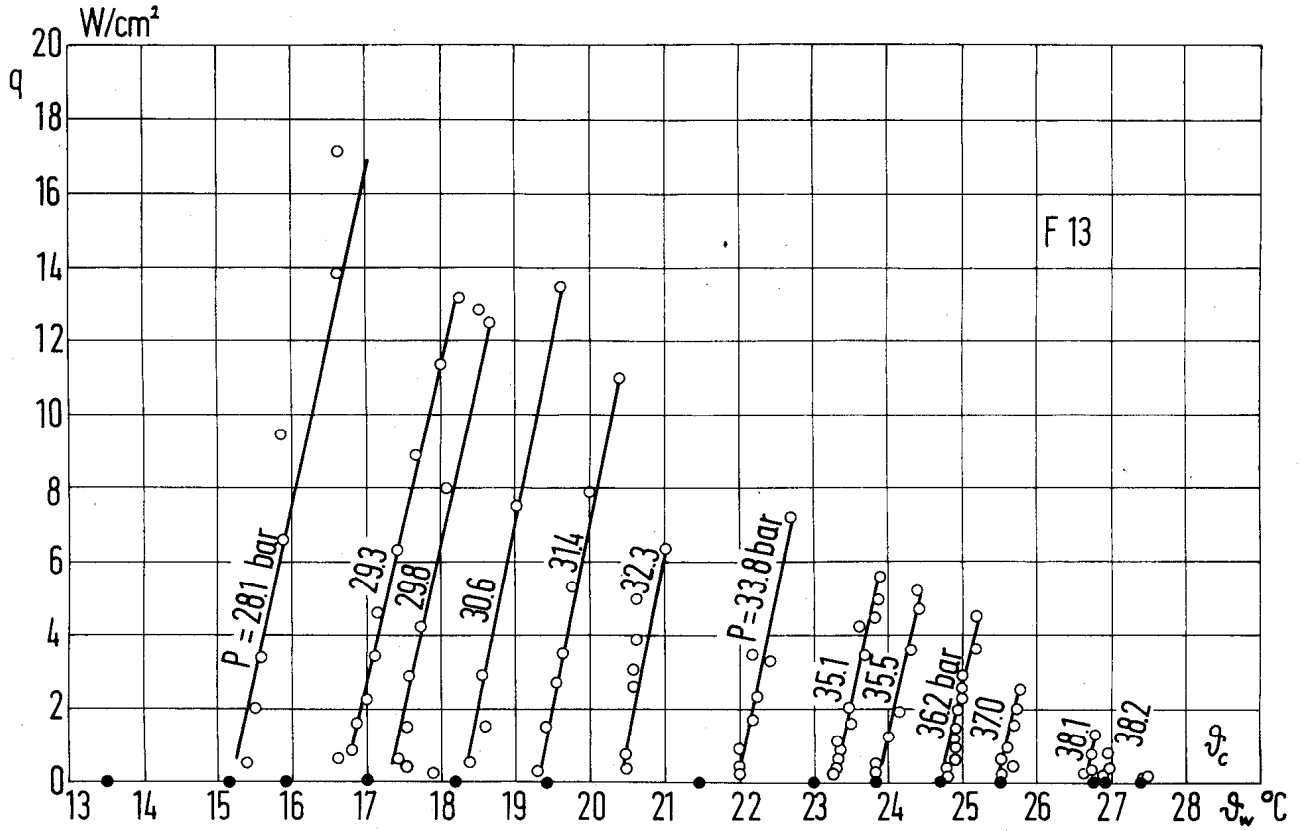

Fig. 8.3. Heat flux density q in nucleate boiling of Freon 13 as a linear function of wire temperature θ_w. Saturation temperatures θ_s are marked as black dots on the abscissa

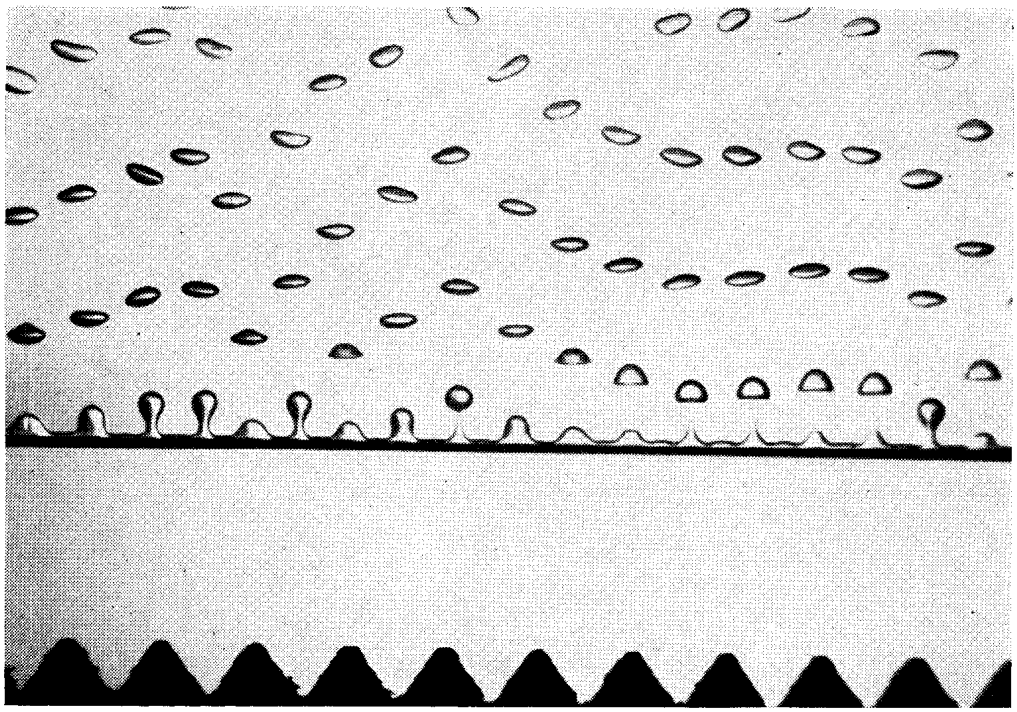

Fig. 8.4. Film boiling of carbon dioxide at $p = 70$ bar, $q = 5{\cdot}2$ W/cm², $\Delta\theta = \theta_w - \theta_s = 19{\cdot}4$ degC

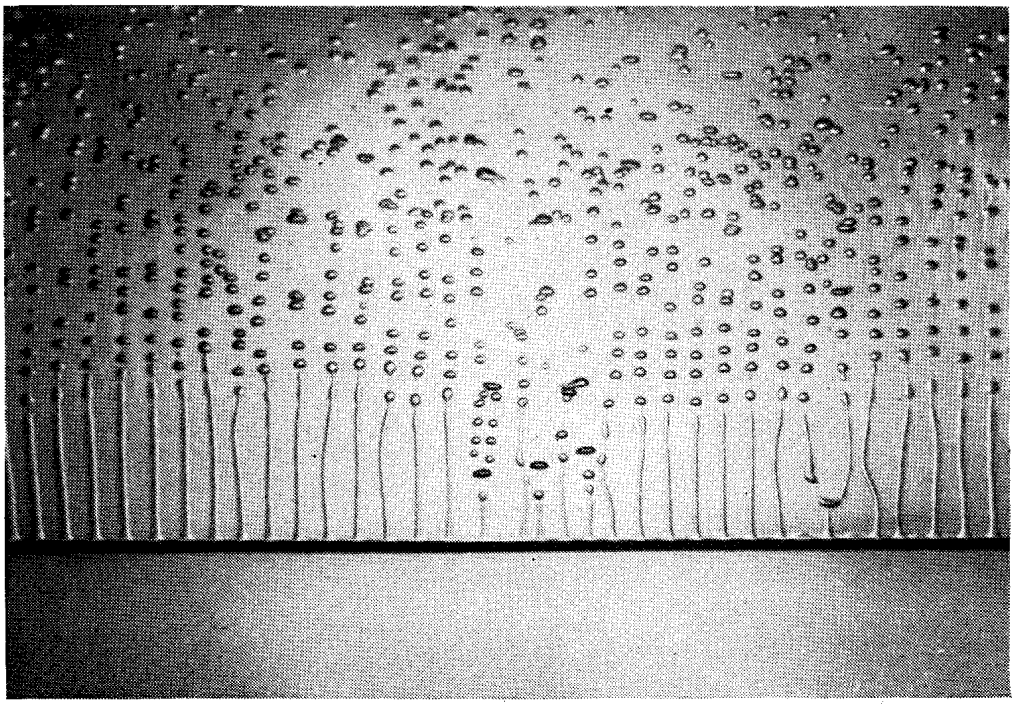

Fig. 8.5. Film boiling of carbon dioxide at $p = 73$ bar, $q = 4{\cdot}8$ W/cm², $\Delta\theta = \theta_w - \theta_s = 14$ degC

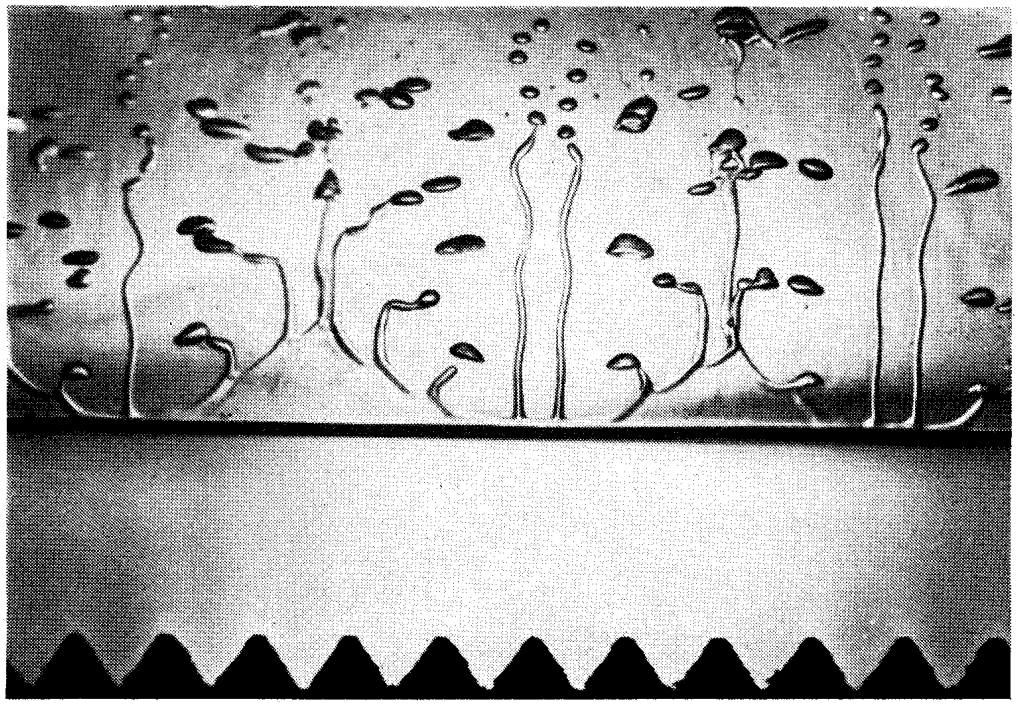

Fig. 8.6. Film boiling of carbon dioxide at $p = 73{\cdot}4$ bar, $q = 5{\cdot}5$ W/cm², $\Delta\theta = \theta_w - \theta_s = 24$ degC

Table 8.1. q_{max} and q_{min} and related values for CO_2 and CF_3Cl

Carbon dioxide (CO_2)

θ_s, °C	q_{max}, W/cm²	q_{min}, W/cm²	M, W/cm²	q_{max}/M	q_{min}/M
20·0	40	17·5	344	0·166	0·051
22·5	32	14	292	0·109	0·055
25·0	23	10	233	0·099	0·043
27·5	14	6	161	0·087	0·037
30·0	4·5	2	79	0·057	0·025
31·0	≈ 0	≈ 0	≈ 0	—	—

Freon 13 (CF_3Cl)

θ_s, °C	q_{max}, W/cm²	q_{min}, W/cm²	M, W/cm²	q_{max}/M	q_{min}/M
10·0	20	11	198	0·101	0·055
15·0	15	8·4	171	0·088	0·049
20·0	9·2	5·5	132	0·068	0·041
25·0	3·5	2	79	0·044	0·025
28·0	≈ 0	≈ 0	≈ 0	—	—

$p/p_c > 0{\cdot}9$ vapour columns are formed with regular distances (Fig. 8.5). These will change into vapour hazes with garland-like boundaries on increasing the heat flux (Fig. 8.6). These highly dissimilar flow patterns do not influence the heat transfer, they are principally of hydrodynamic nature.

MODEL EXPERIMENTS

The flow patterns of rising vapour could be simulated by hydrodynamic model experiments (4) (5). A liquid flowing down a rounded well-wettable edge forms, according to the mass supplied, individual drops in regular distances as shown in Fig. 8.4, or liquid jets which after a certain length break up into drops as displayed in Fig. 8.5. At a still larger liquid flow one consistent film is obtained with constrictions corresponding to the patterns of Fig. 8.6. As in Fig. 8.5, the distances of jets and vapour columns respectively, when related to the Laplace constant $a = [\sigma/g(\rho' - \rho'')]^{1/2}$, are both of the same order of magnitude.

VISUALIZATION

The transition from bubble boiling to film boiling, and vice versa, in addition to various flow patterns of rising vapour, were made visible in a slow-motion film (1200 frames/s) which can be ordered from the Institut für den Wissenschaftlichen Film, 34 Göttingen, Nonnenstieg 72, West Germany, under the number W 792 and the title 'Blasen- und Filmsieden von Kohlendioxid im kritischen Gebiet'.

APPENDIX 8.1

REFERENCES

(1) ZUBER, N. 'Hydrodynamic aspects of boiling heat transfer', AEc tech. Publs AECU-4439, 1959.
(2) KUTATELADZE, S. S. 'Heat transfer in condensation and boiling', AEC-tr-3770, 1959.
(3) BROMLEY, L. A. 'Heat transfer in stable film boiling', *Chem. Engng Prog.* 1950 **46**, 221.
(4) GRIGULL, U. and ABADZIC, E. 'Blasen- und Filmsieden von Kohlendioxid im kritischen Bereich', *Forsch. Ing.-Wesen* 1965 **31**, 27.
(5) GRIGULL, U. 'Photographic investigation of boiling processes in the critical region' (original Russian), Minsk: Science and Technique 1965 in *Heat and Mass Transfer*, Vol. 3: *Heat and mass transfer in change of phase* (eds A. V. Luikov and B. M. Smolski), p. 343.